SUPPLEMENTAL INFORMATION

Ethics Statement

The studies described here have been reviewed and approved by the Animal Care and Use Committees at The University of Chicago and Rutgers, the State University of New Jersey which are both accredited by the Association for Assessment and Accreditation of Laboratory Animal Care (AAALAC).

SUPPLEMENTAL FIGURE LEGENDS

Figure. S1. Characterization of *H2-Ob*-deficient mice generated by CRISPR/Cas9 technology. Related to Figure 4.

(**A**) Western blot analysis of lysates of B cells purified from *H2-Ob*$^{-/-}$, *H2-Ob*$^{+/-}$ and *H2-Ob*$^{+/+}$ mice probed with antibodies against the Oβ luminal domain (top) and β-actin as a loading control (bottom). Purified *H2-Ma*$^{-/-}$ B cells were used as a negative control. Numbers below strain names indicate individual mice. Two independent *H2-Ob*$^{-/-}$ founder mice strains were analyzed. *H2-Ob*$^{-/-}$ mice one and two were derived from founder mouse line 134 and mice three and four were from founder line 4905. Graphs at the bottom show quantification of Oβ levels normalized to the level obtained for *H2-Ob*$^{+/+}$ B cells. Data for *H2-Ob*$^{-/-}$ *mice was combined from both founders.* Results show that *H2-Ob*$^{-/-}$ mice express no detectable Oβ protein and that *H2*-Ob$^{+/-}$ mice express approximately half the level of *H2*-Ob$^{+/+}$ mice. Data are representative of two similar experiments. Significance was calculated using an unpaired *t* test.

(**B**) Representative FACS analysis of spleen cells from *H2-Ob*$^{+/+}$, *H2-Ob*$^{+/-}$ and *H2-Ob*$^{-/-}$ mice (both 134 and 4905 lines were analyzed) showing the frequency of B cells (top plots, defined as B220^{+} CD19^{+}), total dendritic cells (DCs; middle plots, defined as CD11c^{+}) and two DC subsets (bottom plots), CD8α^{+} DCs (defined as CD11c^{+} MHC-II^{+} CD8α^{+} CD205^{+}) and CD8α^{-} DCs (defined as CD11c^{+} MHC-II^{+} CD8α^{-} CD205^{-}). Graphs to right of FACS plots show a

summary of frequencies for all mice analyzed. Data are presented as the frequency of total spleen cells for B cells and total DCs or the frequency in the $CD11c^+$ DC gate for the CD8α DC subsets. Results show that *H2-Ob*-deficiency does not alter antigen presenting cell development since all populations were present at similar frequencies in the spleens of *H2-Ob*$^{+/+}$, *H2-Ob*$^{+/-}$ and *H2-Ob*$^{-/-}$ mice.

Figure S2. MMTV-infected *H2-Oa*- and *H2-Ob*-deficient mice produce virus-neutralizing antibodies. Related to Figure 4.

(**A**) Purified MMTV virions were incubated with the sera from MMTV-infected *H2-Oa*$^{-/-}$ mice and injected i.p. into BALB/cJ mice. Five weeks after injection, mice were bled and peripheral T cells were analyzed by FACS for the percentage of SAg-cognate $CD4^+$T $Vβ6^+$ cells among $CD4^+$ T cells. Their deletion was used as an indicator of virus infectivity. Each dot is a mean of percent of $CD4^+$ $Vβ6^+$ T cells among $CD4^+$ T cells analyzed in three mice injected with the virus incubated with the same serum sample. n, numbers of sera used (combined data with calculated % of neutralization are shown in Figure 4A).

(**B**) Sera from infected *H2-Ob*$^{-/-}$ mice were incubated with purified MMTV(LA) and injected into footpads of BALB/cJ mice. Four days after injection, cells isolated from the draining popliteal lymph node were analyzed by FACS for the percentage of $CD4^+$ $Vβ6^+$ T cells among $CD4^+$ T cells. The proliferation of SAg-cognate T cells was used as indicator of virus infectivity. Each dot is a mean of percent of $CD4^+$ $Vβ6^+$ T cells among $CD4^+$ T cells analyzed in nodes draining the sites of injection with the virus incubated with the same serum. n, number of the sera tested (combined data with calculated % of neutralization are shown in Figure 4B). Sera from infected B6$^{vic1i/i}$ and uninfected B6 (*H2-Oa*$^{+/+}$ and *H2-Ob*$^{+/+}$) were used as positive and negative controls, respectively. Significance was calculated using an unpaired *t* test.

(C) The MMTV-neutralizing capacity of Abs was also tested in offspring produced by MMTV injected females (3 litters from each line). Females from infected *H2-Ob*$^{-/-}$ and B6$^{vic1i/i}$ but not B6 females produced uninfected offspring. n, number of mice screened.

Figure S3. Identification of human *HLA-DOB* variants with altered function. Related to Figure 6.

(**A**) Approach used to measure MHCII-CLIP, DO, DM and MHC-II levels after expression of *HLA-DOB* variants in HeLa.CIITA cells. HeLa cells stably expressing CIITA (MHC-II+, DM+ and low levels of DOA) were transiently transfected with control vectors lacking inserts (IRES-mRuby / IRES-AcGFP) or with only vectors encoding *HLA-DOA*0101* (most common *HLA-DOA* allele; DOA-IRES-mRuby /I RES-AcGFP) or only *HLA-DOB*0101* (most common DOB allele; IRES-mRuby / DOB-IRES-AcGFP) or vectors expressing both *HLA-DOA*0101* and *HLA-DOB*0101* (DOA-IRES-mRuby / DOB-IRES-AcGFP) and 72 hours later cells were surface stained with Abs specific for MHC-II and MHCII-CLIP or fixed, permeabilized and stained with Ab specific for the DO or DM heterodimers followed by flow cytometric analysis. Cells were gated for the expression of mRuby which reports DOA expression and AcGFP which reports DOB expression (Ruby+ GFP+) followed by gating for MHC-II+ cells. MHC-II-CLIP levels were then determined by measuring the gMFI for the Ruby+ GFP+ MHC-II+ cells (top). For the determination of DO levels, cells were gated for mRuby and AcGFP followed by the selection of DM+ cells and the DO gMFI was determined in these cells (Ruby+ GFP+ DM+) (bottom). Fixation of cells results in decreased mRuby and AcGFP fluorescence. The gMFI fluorescence levels for MHC-II-CLIP and DO are indicated on the left side of the respective histograms. DO expression and increased MHC-II-CLIP levels were observed only after transfection of vectors expressing both *HLA-DOA* and *HLA-DOB*. Data is representative of 5 similar experiments.

(**B**) MHC-II-CLIP, DO, DM and MHC-II levels after expression of the 32 *HLA-DOB* variants in HeLa.CIITA cells. HeLa.CIITA cells were transiently transfected with a vector expressing *HLA-DOA*0101* (DOA-IRES-mRuby) together with vectors expressing one of the 32 *HLA-DOB* variants and analyzed as in panel S3A. The gMFI for MHC-II-CLIP, DO, DM and MHC-II for each DOB variant were determined and normalized to the gMFI value obtained after transfection of *HLA-DOA*0101* and *HLA-DOB*0101*. Seven of the *HLA-DOB* variants were frameshift and stop mutants and did not produce detectable DOβ (see also Figure S4A). Thus, the average gMFI obtained for MHCII-CLIP and DO was subtracted from the gMFI values obtained for the other 25 DOB variants to remove background staining prior to normalization with the gMFI obtained for DOβ*0101. The DOB variant transfected is indicated on the Y-axis of each graph and the relative expression of MHC-II-CLIP, DO, DM and MHC-II is indicated on the X-axis. Open circles represent results from individual experiments and bars represent the mean +/- SD. Data was combined from 3-4 individual experiments.

Figure S4. Frameshift and stop codon DOB variants do not make functional DOB protein and detailed analysis of DOB G77V. Related to Figure 6.

(**A**) Western blot analysis of lysates from Hela.CIITA cells transiently transfected with vectors encoding for *HLA-DOA*0101* and the indicated *HLA-DOB* alleles were probed with antibodies specific for the cytoplasmic tails of DOβ (top) and DMβ (middle) or β-actin as a loading control (bottom). Transfection with *HLA-DOA*0101* and *HLA-DOB*0101* was used as a positive control. Data are representative of 3 similar experiments.

(**B**) Differences in ability of DOB*0101 and DOB G77V to suppress DM function. HeLa.CIITA cells transfected with plasmids encoding *HLA-DOA*0101* and *HLA-DOB*0101* or the *HLA-DOB* G77V variant were surface stained for MHC-II and MHC-II-CLIP followed by analysis by flow cytometry. Resulting plots were analyzed by gating for mRuby expressing cells, which reports DOα expression and then for MHC-II (not shown). AcGFP levels (reports DOβ expression) in the mRuby+ MHC-II+ cells were divided into bins (1-5) based upon fluorescence as indicated and the gMFI for MHC-II-CLIP in each bin was determined and plotted in bar graphs below each FACs plot. To determine DO levels relative to AcGFP expression, transfected cells that had been fixed and permeablized prior to staining with Abs to DO and DM were analyzed by flow cytometry. Note that fixation of cells results in decreased mRuby and AcGFP fluorescence. Analysis was performed by gating on mRuby+ cells followed by selecting DM expressing cells (not shown). AcGFP levels in the mRuby+ DM+ cells were divided into bins (1-5) as described above and DO gMFI for each bin was plotted in bar graphs below each FACs plot. Staining is representative of 5 individual experiments.

Figure S5. Amino acid alignment of DOβ common alleles and variants. Related to Figure 6.

Alignment of the five common DOβ alleles to DOB*0101. Dashes indicate similarity. Missense, frameshift and stop mutations for the other 27 DOB variants are indicated below the amino acid sequences for the common variants. DOβ alleles with altered function are highlighted in the same colors used in Figures 6, 7 and S3B. DOβ protein domains are marked by colored frames.

Figure S6. A heatmap of pairwise linkage disequilibrium statistics within the MHC-II region. Related to Figure 6.

Data from all populations in 1000 Genomes Project was used to calculate D' scores, ranging from red indicating D'=1 to white indicating D'=0. Variants are ordered by genomic coordinates. Note that rs9276370, rs7756516, rs7453920, rs144814623, and rs2071469 all exhibit pairwise D' > .5, suggesting they are significantly associated with each other. rs9276370, rs7756516 and rs7453920 span the region linked to persistent HBV infection (Chang et al., 2014) whereas a 'C' allele in rs2071469 mapped to the 5' UTR of DOB was significantly associated with increased susceptibility to HCV infection (Huang et al., 2015). An 'A' allele in coding rs144814623 (resulting in DOβ G77V) was found in linkage disequilibrium with a 'C' in rs 4273729, the latter SNP was associated with HCV persistence (Duggal et al., 2013). Genes in the MHC-II region, their intron–exon structure, and genomic coordinates (in Mb, using the NCBI human genome sequence, Build 37, as reference) are shown at the bottom. Coding rs144814623 and non-coding 5'UTR-specific rs2071469 are within the DOB gene.

Figure S7. I/LnJ Oβ is a full-length protein which is produced at normal levels and interacts with DM in endosomal compartments. Related to Figure 7.

(A) Quantification of Oβ and H2-Mα levels using western blotting (as shown in Figure 7A). Normalization was performed relative to β-actin levels. Data are presented as the protein level relative to that obtained for B6 B cells. Data combined from 4 independent experiments. Significance was calculated using an unpaired *t* test. n, number of mice.
(B) Expression of C-terminal B6 or I/LnJ Oβ-YFP fusion proteins (YFP served as control) was measured 48 hrs after transfection in L-CIITA cells. CIITA expression allowed for endogenous expression of Mα, Mβ and Oα but not Oβ. Lysates were analyzed by western

blotting with antibodies specific for the Oβ luminal domain (top), YFP (middle) or Mα (bottom). Results show that the faster migration of I/LnJ Oβ after electrophoresis on SDS-PAGE gels is not due to premature protein truncation since full length I/LnJ fusion protein was detected. Data are representative of 5 independent experiments. *, a non-specific band.

(C) Western blot analysis of *in vitro* transcribed and translated (TnT) B6 and I/LnJ Oβ (left) or post-nuclear supernatants from B6 or I/LnJ splenocytes (right) separated by 10% SDS-PAGE (top) or by 10% SDS-PAGE containing 8M urea (bottom). Blots were probed with Abs specific for the Oβ luminal domain. TnT of an empty vector (pTnT) and *H2-Oa*$^{-/-}$ splenocytes were used as negative controls for the respective blots. Triangles indicate titrated doses of the TnT generated samples loaded on the gel.

(D) Left panel, I/LnJ Oβ traffics from the ER. H2-M and co-associated H2-O immunoprecipitated from the lysates of purified B6, I/LnJ, and *H2-Ob*$^{-/-}$ (negative control) splenic B cells were released from the immunoprecipitation pellets and treated with Endo H (+Endo H) or Peptide-*N*-Glycosidase F (+PNGase F) prior to analysis by western blotting with Abs specific for Oβ luminal domain. B6 and I/LnJ Oβ were both resistant to digestion with Endo H but not PNGase F (which cleaves off immature and mature glycans). Thus, I/LnJ Oβ trafficked from the ER to post-golgi compartments. **Right panel**, H2-O is an obligate heterodimer: in the absence of Oα, Oβ never traffics from the ER and therefore remains sensitive to digestion with Endo H. We used the sensitivity of Oβ to Endo H digestion as a control to show that the Endo H used in experiments presented in the left panel was active. For these experiments, Oβ was immunoprecipitated from detergent lysates of *H2-Oa*$^{-/-}$ or *H2-Ob*$^{-/-}$ (negative control) B cells using a monoclonal Ab specific for Oβ. Oβ was released from the immunoprecipitation pellet and equal aliquots were treated with Endo H or PNGase F or mock treated (mock) prior to analysis by western blotting with

Abs specific for the Oβ luminal domain. As expected Oβ in *H2-Oa*$^{-/-}$ B cells remained sensitive to Endo H digestion since Endo H- and PNGase F-digested Oβ migrated faster on SDS-PAGE than the mock treated Oβ. Oβ^{glycos}, glycosylated Oβ; Oβ^{deglycos}, deglycosylated Oβ. * and ** mark non-specific bands. Data are representative of 2 independent experiments.

Table S1. Nonsynonymous single nucleotide variants (SNV), deletions or insertions found in the *vic1* critical region. Related to Figure 3. Comparison between the B6 and I/LnJ genomes. NT, nucleotide. POS, position (nts).

Table S2. Nonsynonymous single nucleotide variants (SNV), deletions or insertions found in the *vic1* critical region. Related to Figure 3. Comparison between the B6 and BALB/cJ genomes. NT, nucleotide. POS, position (nts).

Table S3. Nonsynonymous single nucleotide variants (SNV), deletions or insertions found in the *vic1* critical region. Related to Figure 3. Comparison between the B6 and C3H/HeN genomes. NT, nucleotide. POS, position (nts).

Table S4. Human *HLA-DOB* alleles. Related to Figure 6 and 7. RSID, SNP ID. Highlighted are alleles which have been studied.

Table S5. Human *HLA-DOA* alleles. Related to Figure 6 and 7. RSID, SNP ID

REFERENCES

Acha-Orbea, H., and MacDonald, H.R. (1995). Superantigens of mouse mammary tumor virus. Annu Rev Immunol *13*, 459-486.

Buggiano, V., Goldman, A., Nepomnaschy, I., Bekinschtein, P., Berguer, P., Lombardi, G., Deroche, A., Francisco, M.V., and Piazzon, I. (1999). Characterization of two infectious mouse mammary tumour viruses: superantigenicity and tumorigenicity. Scand J Immunol *49*, 269-277.

Case, L.K., Petell, L., Yurkovetskiy, L., Purdy, A., Savage, K.J., and Golovkina, T.V. (2008). Replication of beta- and gammaretroviruses is restricted in I/LnJ mice via the same genetic mechanism. Journal of virology *82*, 1438-1447.

Chang, S.W., Fann, C.S., Su, W.H., Wang, Y.C., Weng, C.C., Yu, C.J., Hsu, C.L., Hsieh, A.R., Chien, R.N., Chu, C.M.*, et al.* (2014). A genome-wide association study on chronic HBV infection and its clinical progression in male Han-Taiwanese. PLoS One *9*, e99724.

Chirgwin, J.M., Prxybyla, A.E., MacDonald, R.J., and Rutter, W.J. (1979). Isolation of biologically active ribonucleic acid from sources enriched in ribonuclease. Biochemistry *18*, 5294-5299.

de Vries, W.N., Binns, L.T., Fancher, K.S., Dean, J., Moore, R., Kemler, R., and Knowles, B.B. (2000). Expression of Cre recombinase in mouse oocytes: a means to study maternal effect genes. Genesis *26*, 110-112.

Dembic, Z., Ayane, M., Klein, J., Steinmetz, M., Benoist, C.O., and Mathis, D.J. (1985). Inbred and wild mice carry identical deletions in their E alpha MHC genes. EMBO J *4*, 127.

Denzin, L.K., Robbins, N.F., Carboy-Newcomb, C., and Cresswell, P. (1994). Assembly and intracellular transport of HLA-DM and correction of the class II antigen-processing defect in T2 cells. Immunity *1*, 595-606.

Denzin, L.K., Sant'Angelo, D.B., Hammond, C., Surman, M.J., and Cresswell, P. (1997). Negative regulation by HLA-DO of MHC class II-restricted antigen processing. Science *278*, 106-109.

Duggal, P., Thio, C.L., Wojcik, G.L., Goedert, J.J., Mangia, A., Latanich, R., Kim, A.Y., Lauer, G.M., Chung, R.T., Peters, M.G.*, et al.* (2013). Genome-wide association study of spontaneous resolution of hepatitis C virus infection: data from multiple cohorts. Ann Intern Med *158*, 235-245.

Fallas, J.L., Tobin, H.M., Lou, O., Guo, D., Sant'Angelo, D.B., and Denzin, L.K. (2004). Ectopic expression of HLA-DO in mouse dendritic cells diminishes MHC class II antigen presentation. J Immunol *173*, 1549-1560.

Fallas, J.L., Yi, W., Draghi, N.A., O'Rourke, H.M., and Denzin, L.K. (2007). Expression patterns of H2-O in mouse B cells and dendritic cells correlate with cell function. J Immunol *178*, 1488-1497.

Finke, D., Luther, S.A., and Acha-Orbea, H. (2003). The role of neutralizing antibodies for mouse mammary tumor virus transmission and mammary cancer development. Proceedings of the National Academy of Sciences of the United States of America *100*, 199-204.

Glazier, K.S., Hake, S.B., Tobin, H.M., Chadburn, A., Schattner, E.J., and Denzin, L.K. (2002). Germinal center B cells regulate their capability to present antigen by modulation of HLA-DO. J Exp Med *195*, 1063-1069.

Golovkina, T.V., Piazzon, I., Nepomnaschy, I., Buggiano, V., de Olano Vela, M., and Ross, S.R. (1997). Generation of a tumorigenic milk-borne mouse mammary tumor virus by recombination between endogenous and exogenous viruses. J Virol *71*, 3895-3903.

Hammond, C., Denzin, L.K., Pan, M., Griffith, J.M., Geuze, H.J., and Cresswell, P. (1998). The tetraspan protein CD82 is a resident of MHC class II compartments where it associates with HLA-DR, -DM, and -DO molecules. J Immunol *161*, 3282-3291.

Hashimoto, K., Joshi, S.K., and Koni, P.A. (2002). A conditional null allele of the major histocompatibility IA-beta chain gene. Genesis *32*, 152-153.

Hook, L.M., Jude, B.A., Ter-Grigorov, V.S., Hartley, J.W., Morse, H.C., 3rd, Trainin, Z., Toder, V., Chervonsky, A.V., and Golovkina, T.V. (2002). Characterization of a novel murine retrovirus mixture that facilitates hematopoiesis. Journal of virology *76*, 12112-12122.

Huang, P., Zhang, Y., Lu, X., Xu, Y., Wang, J., Zhang, Y., Yu, R., and Su, J. (2015). Association of polymorphisms in HLA antigen presentation-related genes with the outcomes of HCV infection. PLoS One *10*, e0123513.

Janeway, C.A., Jr., Conrad, P.J., Lerner, E.A., Babich, J., Wettstein, P., and Murphy, D.B. (1984). Monoclonal antibodies specific for Ia glycoproteins raised by immunization with activated T cells: possible role of T cellbound Ia antigens as targets of immunoregulatory T cells. J Immunol *132*, 662-667.

Kane, M., Case, L.K., Wang, C., Yurkovetskiy, L., Dikiy, S., and Golovkina, T.V. (2011). Innate Immune Sensing of Retroviral Infection via Toll-like Receptor 7 Occurs upon Viral Entry. Immunity *35*, 135-145.

Khalil, H., Deshaies, F., Bellemare-Pelletier, A., Brunet, A., Faubert, A., Azar, G.A., and Thibodeau, J. (2002). Class II transactivator-induced expression of HLA-DO(beta) in HeLa cells. Tissue Antigens *60*, 372-382.

Langmead, B., and Salzberg, S.L. (2012). Fast gapped-read alignment with Bowtie 2. Nature methods *9*, 357-359.

Liljedahl, M., Winqvist, O., Surh, C.D., Wong, P., Ngo, K., Teyton, L., Peterson, P.A., Brunmark, A., Rudensky, A.Y., Fung-Leung, W.P*., et al.* (1998). Altered antigen presentation in mice lacking H2-O. Immunity *8*, 233-243.

Logunova, N.N., Viret, C., Pobezinsky, L.A., Miller, S.A., Kazansky, D.B., Sundberg, J.P., and Chervonsky, A.V. (2005). Restricted MHC-peptide repertoire predisposes to autoimmunity. J Exp Med *202*, 73-84.

Machiela, M.J., and Chanock, S.J. (2015). LDlink: a web-based application for exploring population-specific haplotype structure and linking correlated alleles of possible functional variants. Bioinformatics *31*, 3555-3557.

Madsen, L., Labrecque, N., Engberg, J., Dierich, A., Svejgaard, A., Benoist, C., Mathis, D., and Fugger, L. (1999). Mice lacking all conventional MHC class II genes. Proceedings of the National Academy of Sciences of the United States of America *96*, 10338-10343.

Miyazaki, T., Wolf, P., Tourne, S., Waltzinger, C., Dierich, A., Barois, N., Ploegh, H., Benoist, C., and Mathis, D. (1996). Mice lacking H2-M complexes, enigmatic elements of the MHC class II peptide-loading pathway. Cell *84*, 531-541.

Oi, V.T., Jones, P.P., Goding, J.W., Herzenberg, L.A., and Herzenberg, L.A. (1978). Properties of monoclonal antibodies to mouse Ig allotypes, H-2, and Ia antigens. Curr Top Microbiol Immunol *81*, 115-120.

Piazzon, I., Goldman, A., Torello, S., Nepomnaschy, I., Deroche, A., and Dran, G. (1994). Transmission of an Mls-1a-like superantigen to BALB/c mice by foster-nursing on F1 Mls-1bxa mothers. Sex-influenced onset of clonal deletion. J Immunol *153*, 1553-1562.

Purdy, A., Case, L., Duvall, M., Overstrom-Coleman, M., Monnier, N., Chervonsky, A., and Golovkina, T. (2003). Unique resistance of I/LnJ mice to a retrovirus is due to sustained interferon gamma-dependent production of virus-neutralizing antibodies. J Exp Med *197*, 233-243.

Robbins, N.F., Hammond, C., Denzin, L.K., Pan, M., and Cresswell, P. (1996). Trafficking of major histocompatibility complex class II molecules through intracellular compartments containing HLA-DM. Hum Immunol *45*, 13-23.

Rowe, W.P., Pugh, W.E., and Hartley, J.W. (1970). Plaque assay techniques for murine leukemia viruses. Virology *42*, 1136-1139.

Vugmeyster, Y., Glas, R., Perarnau, B., Lemonnier, F.A., Eisen, H., and Ploegh, H. (1998). Major histocompatibility complex (MHC) class I KbDb -/- deficient mice

possess functional CD8+ T cells and natural killer cells. Proceedings of the National Academy of Sciences of the United States of America *95*, 12492-12497.

Wang, K., Li, M., and Hakonarson, H. (2010). ANNOVAR: functional annotation of genetic variants from high-throughput sequencing data. Nucleic acids research *38*, e164.

Yalcin, B., Wong, K., Bhomra, A., Goodson, M., Keane, T.M., Adams, D.J., and Flint, J. (2012). The fine-scale architecture of structural variants in 17 mouse genomes. Genome biology *13*, R18.

Zhou, S., Kurt-Jones, E.A., Cerny, A.M., Chan, M., Bronson, R.T., and Finberg, R.W. (2009). MyD88 intrinsically regulates CD4 T-cell responses. Journal of virology *83*, 1625-1634.

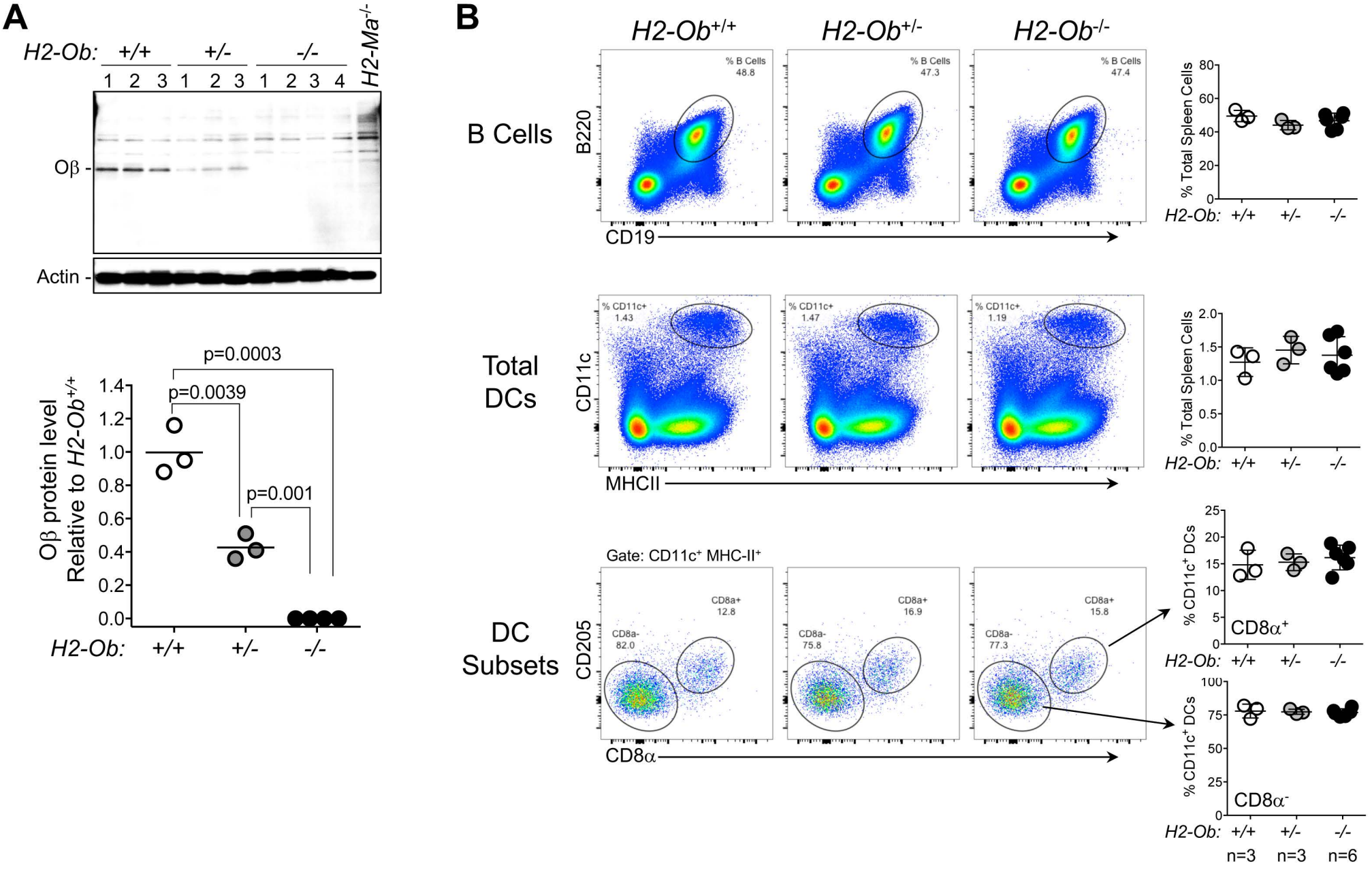

Figure S1 related to Figure 4

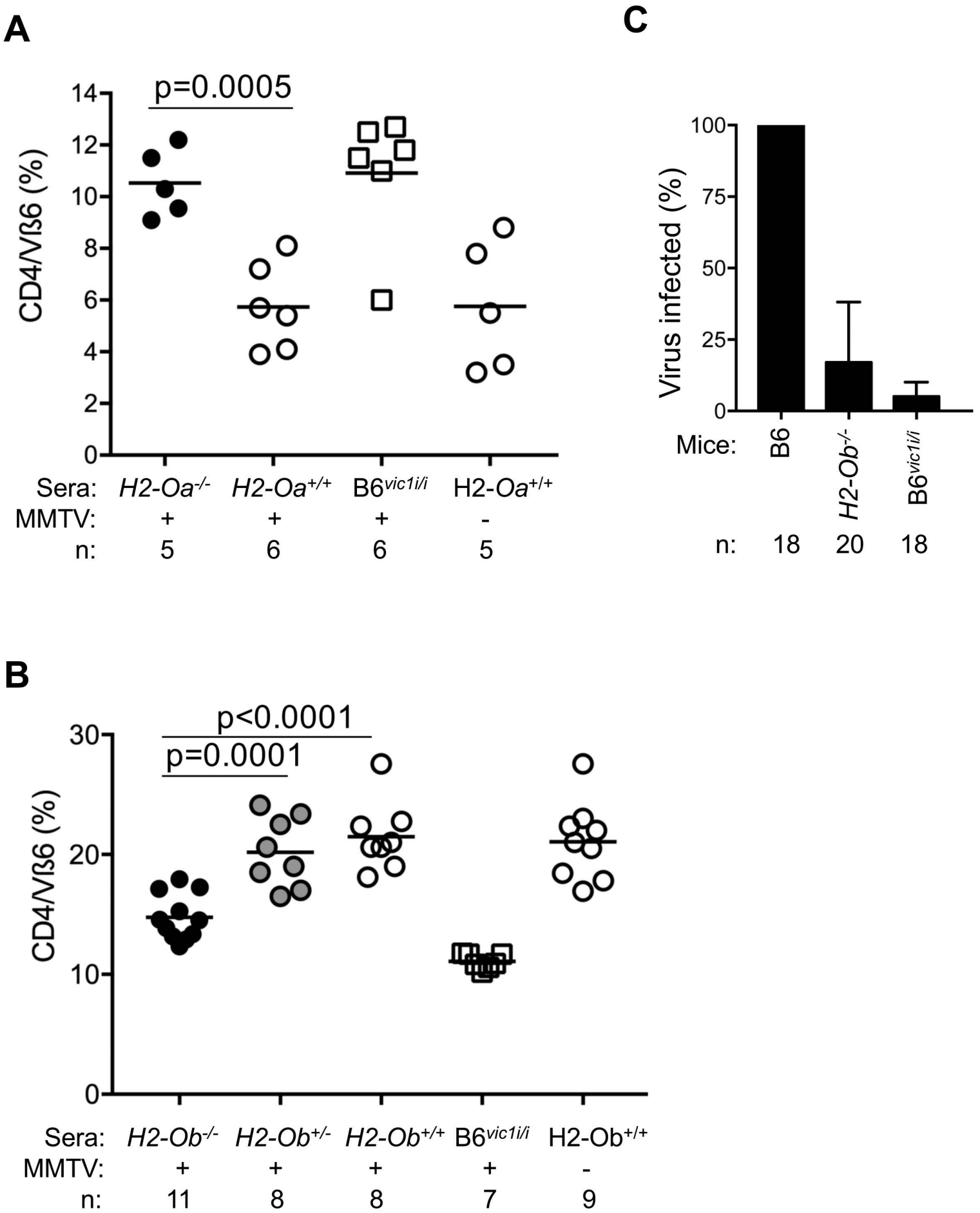

Figure S2 related to Figure 4

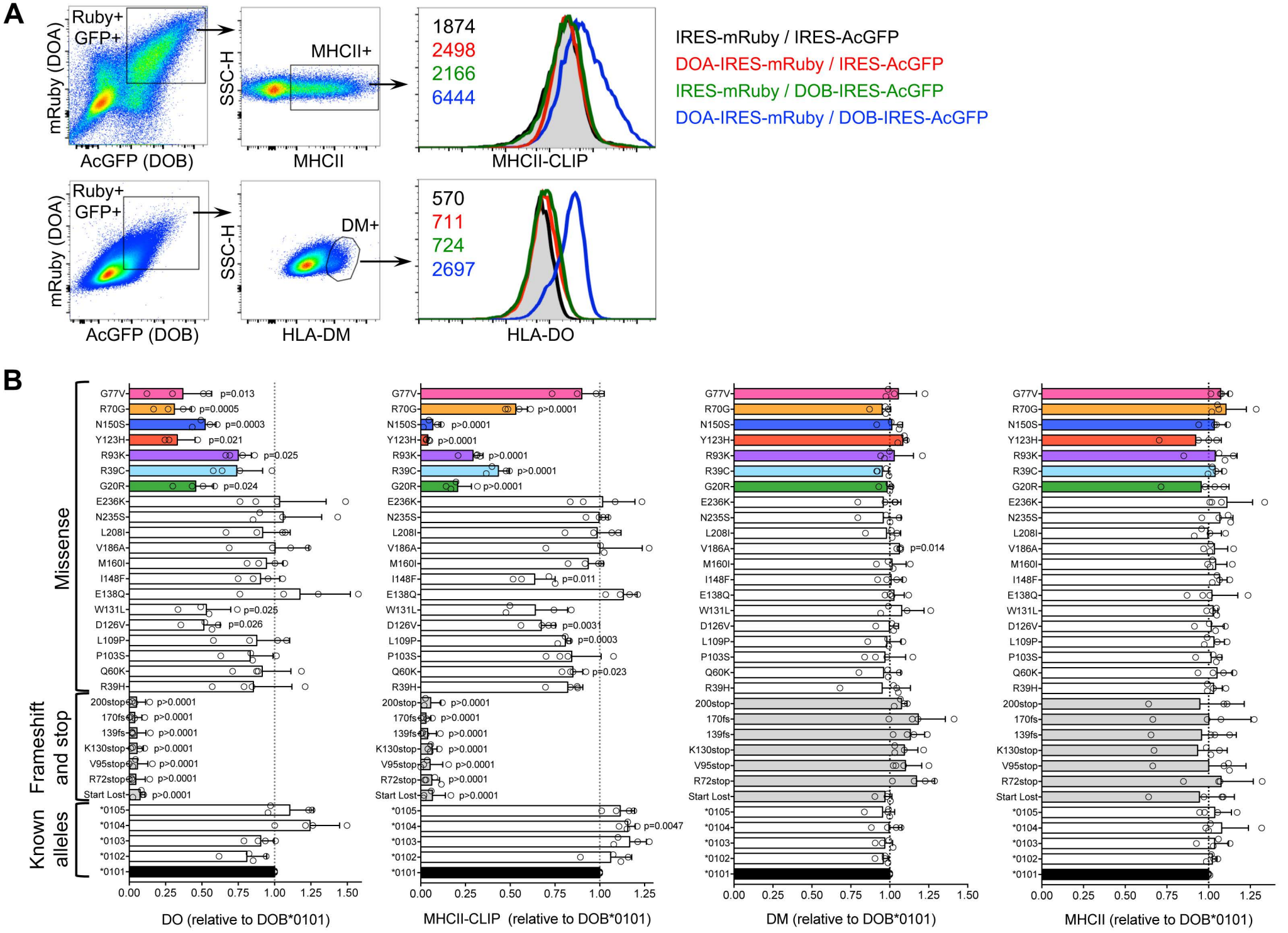

Figure S3 related to Figure 6

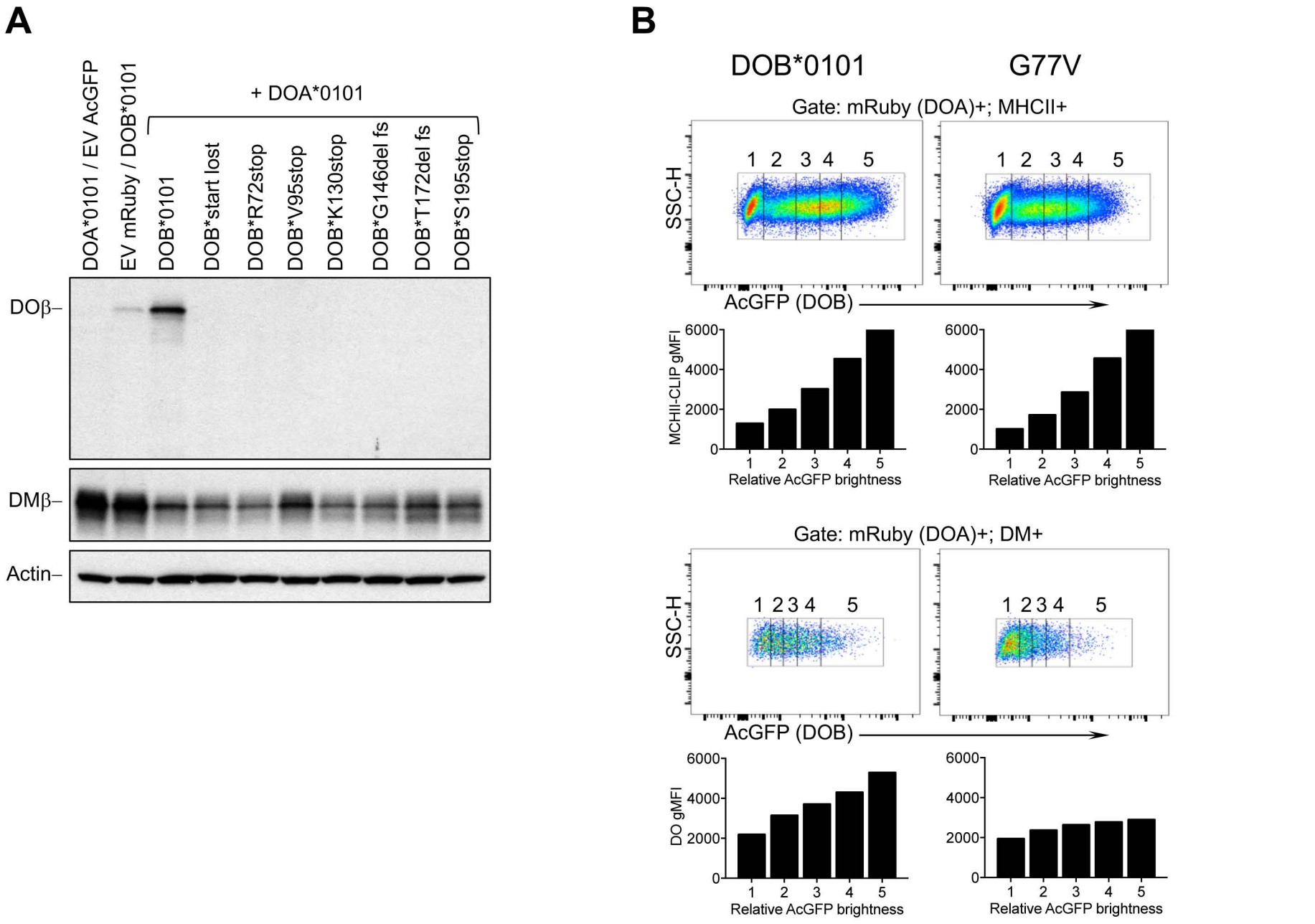

Figure S4 related to Figure 6

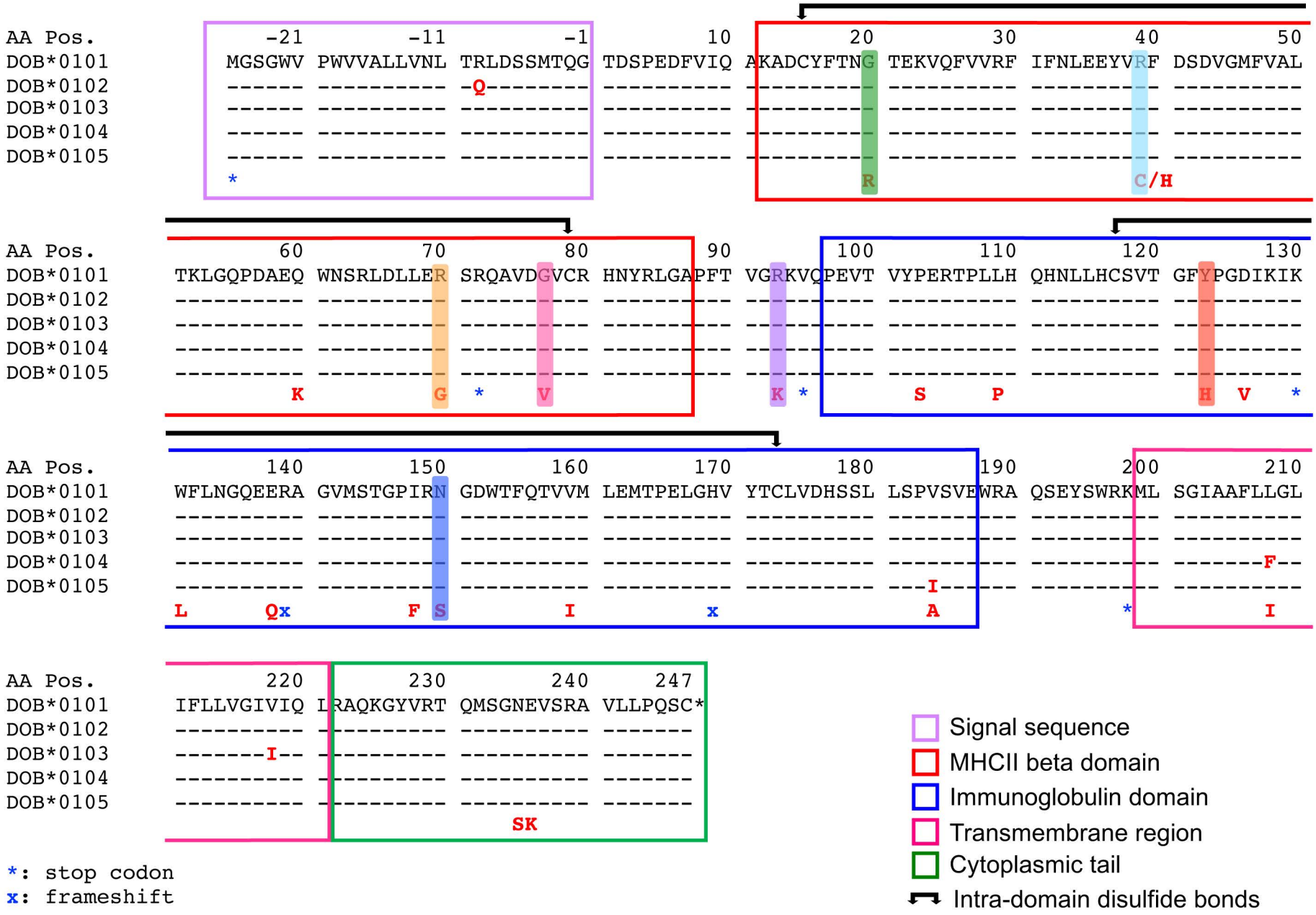

Figure S5 related to Figure 6

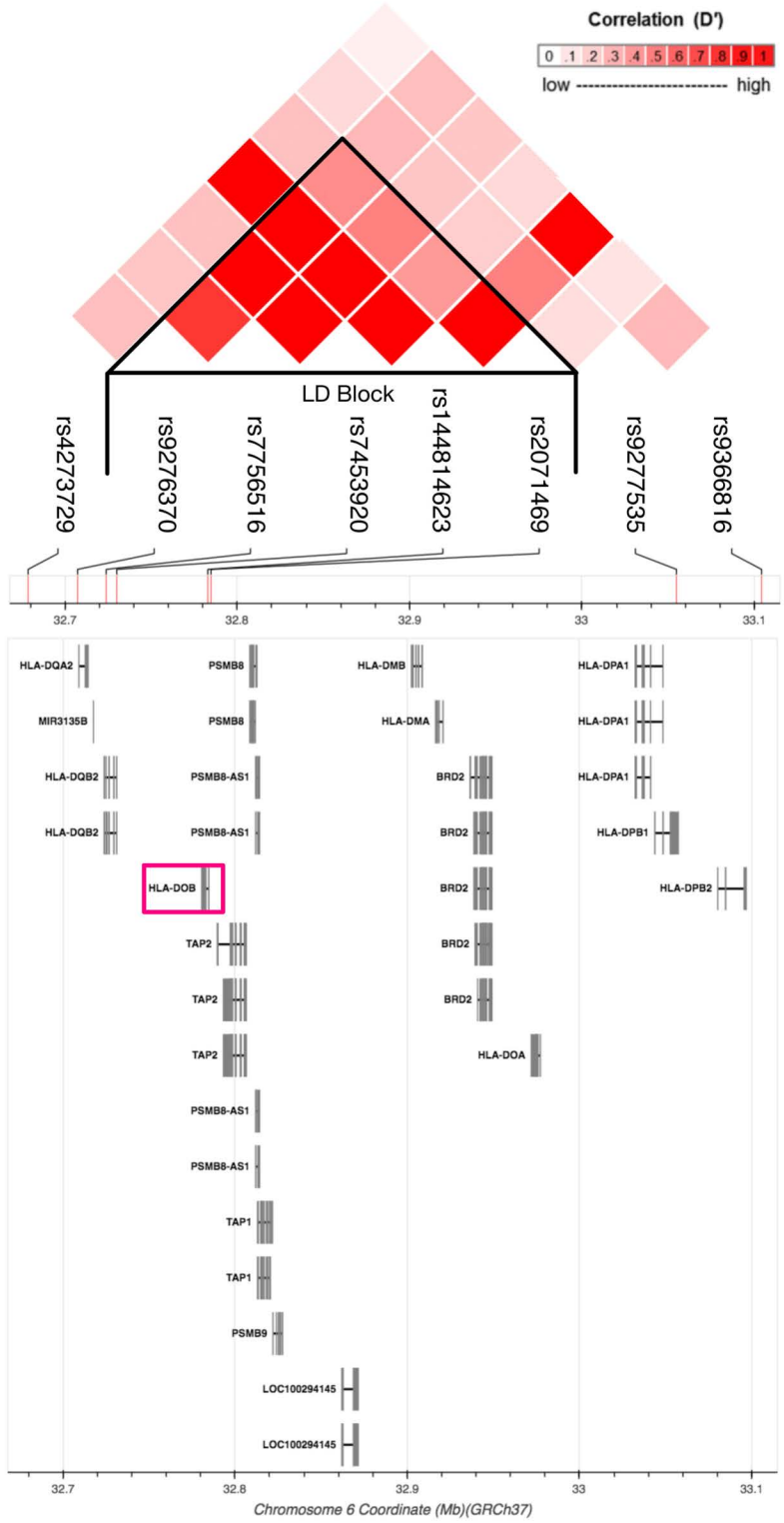

Figure S6 related to Figure 6

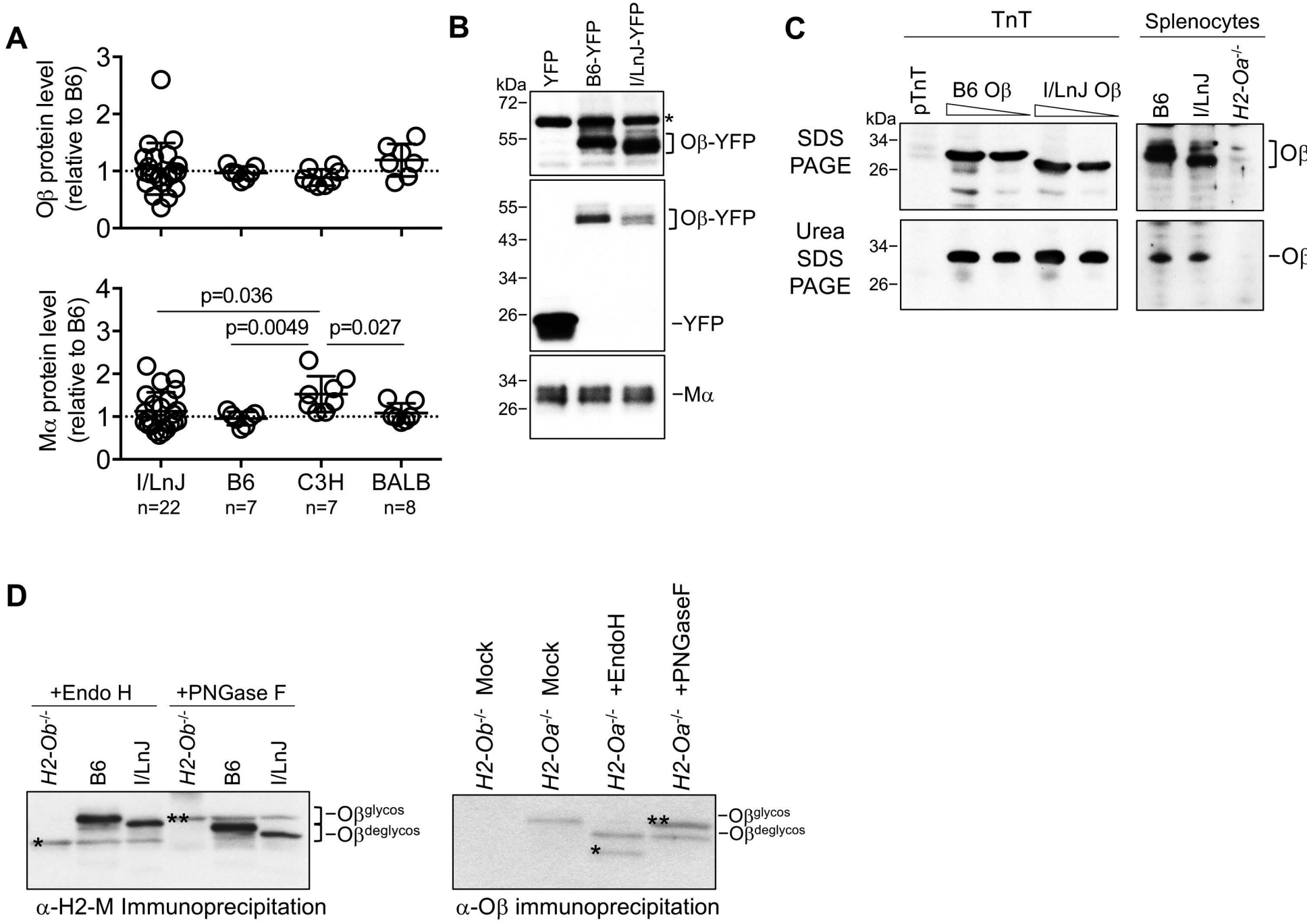

Figure S7 related to Figure 7